SANDIA REPORT

SAND88—0190 • TTC—0780 • UC—71
Unlimited Release
Printed February 1988

Sample Problem Manual For Benchmarking of Cask Analysis Codes

Robert E. Glass

Prepared by
Sandia National Laboratories
Albuquerque, New Mexico 87185 and Livermore, California 94550
for the United States Department of Energy
under Contract DE-AC04-76DP00789

SF2900Q(8-81)

Issued by Sandia National Laboratories, operated for the United States Department of Energy by Sandia Corporation.

Printed in the United States of America
Available from
National Technical Information Service
U.S. Department of Commerce
5285 Port Royal Road
Springfield, VA 22161

NTIS price codes
Printed copy: A03
Microfiche copy: A01

SAND88-0190
TTC-0780
Unlimited Release

Distribution
Category UC-71

SAMPLE PROBLEM MANUAL FOR BENCHMARKING OF CASK ANALYSIS CODES*

Robert E. Glass
Transportation Systems Technology and
Analysis Division 6322
Sandia National Laboratories**
Albuquerque, NM 87185

SAND--88-0190

DE88 006596

ABSTRACT

A series of problems have been defined to evaluate structural and thermal codes. These problems were designed to simulate the hypothetical accident conditions given in Title 10 of the Code of Federal Regulation, Part 71 (10CFR71) while retaining simple geometries. This produced a problem set that exercises the ability of the codes to model pertinent physical phenomena without requiring extensive use of computer resources.

The solutions that are presented are consensus solutions based on computer analyses done by both national laboratories and industry in the United States, United Kingdom, France, Italy, Sweden, and Japan.

The intent of this manual is to provide code users with a set of standard structural and thermal problems and solutions which can be used to evaluate individual codes.

*This work performed at Sandia National Laboratories, Albuquerque, New Mexico, supported by the U. S. Department of Energy under Contract DE-AC04-76DP00789

**A United States Department of Energy Facility

TABLE OF CONTENTS

TABLES

FIGURES

1.0 Introduction

An issue of significant concern in nuclear waste management is the ability of computer codes to correctly simulate the phenomena associated with the transport of radioactive materials. In particular, structural, thermal, criticality, and shielding codes must be able to simulate normal transport and hypothetical accident conditions and the corresponding package response in order to design and certify packages based on analysis.

The United States Department of Energy is funding programs to provide analytical code benchmarks and to evaluate the many codes used in the design and certification of casks. This report contains those problems and solutions developed for evaluating structural and thermal codes.

This effort is in conjunction with code intercomparisons being done under the auspices of the Organization for Economic Cooperation and Development (OECD) Nuclear Energy Agency Committee on Reactor Physics (CRP) and Committee on the Safety of Nuclear Installations (CSNI). A standard criticality benchmark problem set has been completed (1) for the OECD. Similar efforts are underway in the areas of thermal (2) and shielding analysis.

These code comparison efforts are complemented with experimental programs at Sandia National Laboratories, which will provide data for comparison with numerical results. The remainder of this report presents the existing structural and thermal problems for which consensus solutions are available.

In 1982 Sandia undertook the task of developing a set of standard problems to be used in the evaluation of codes used in the design and certification of radioactive materials transportation packages. These problems were developed with the Battelle Pacific Northwest Laboratories. These problems were presented at the first Industry/Government Joint Code Information Exchange (3) in November 1982. At that meeting both government and industry participants were asked to provide solutions and input to the program.

These solutions were compiled and presented to the participants at the second Industry/Government Joint Code Information Exchange (4) in October 1984. The participants were asked to comment on the existing problem set and to provide input for an expanded problem set.

Based on the results of the second information exchange, Sandia developed a proposal for the international intercomparison of thermal codes to be hosted by the Organization for Economic Cooperation and Development (OECD). The heat transfer working group that was subsequently established has completed the definition and analysis of the thermal problem set.

Each problem set and the corresponding solutions (5, 6) have been incorporated into the sample problems contained in this document.

The constraints on the development of the problems were that they should be cask-like in nature, address a regulatory condition, and be as geometrically simple as possible.

These problems are intended to be used to evaluate the ability of codes to simulate realistic physical phenomena. They are not all inclusive. The problems do not address cask specific structural phenomena, such as crushing of impact limiters or buckling of fins. Cask specific thermal phenomena not addressed include phase change and natural convection. These problems do encompass the phenomena encountered in the analysis of casks, such as conduction, radiation, and a specified convective boundary.

The solutions that are presented are a consensus of the individual solutions. They are representative of the codes currently available for these types of analysis. In all cases the solutions have been reviewed by all participants, and only those agreed on have been included in this document. When a closed form analytical solution is available, it is also presented.

2.0 Structural Problems

The structural problems simulate the 30-foot free drop specified in Title 10 of the Code of Federal Regulations, Part 71 (10CFR71). The regulations define the free drop as "A free drop through a distance of nine m (30 ft.)

onto a flat, essentially unyielding, horizontal surface." This definition results in an initial impact velocity of 13.41 m/s (528 ips) and defines the impact boundary. These initial and boundary conditions are used in each of the structural problems. End and side impact problems are presented.

To completely model radioactive materials shipping casks, both elastic and inelastic response may be modeled. The U. S. Nuclear Regulatory Commission's Regulatory Guide 7.6 requires essentially elastic behavior of the containment boundary. There are, however, regions of the cask which will experience plastic deformation, either in an impact limiting component or during the puncture event. For these reasons the problems include both elastic only and elastic/plastic deformations.

Included in the solutions are gross cask body behavior, such as impact durations, rebound velocities, and total plastic deformations. For the elastic problems selected stresses are presented as a function of time. The tabular data include means and standard deviations. The graphical data presented envelops the numerical solutions.

The impact duration provides a check on the ability of codes to propagate the compressive stress wave. For an elastic response the impact duration is equal to the distance through which the wave is propagated divided by the wave speed.

The rebound velocity is a check on the code's conservation of energy. For an elastic response the impact and rebound velocities should be equal since no energy is dissipated. In an elastic/plastic impact, the rebound velocity is lessened according to the amount of energy dissipated in plastic deformation.

Gross plastic deformations (final axial deformation and ovalization) are used to evaluate the code's ability to predict nonlinear behavior. This is essential in predicting the postaccident configuration and, in particular, determining permanent deformation of the sealing surface.

Stress plots are required to determine the ability of codes to predict localized response. In cask design this determines potential problem areas or potential failure initialization zones.

The codes used were HONDOII (7), HONDOIII (8), MANJUSRI-2D, PISCES-2DELK, ANSYS (9), ABAQUS (10), and DYNA2D (11). These codes include both finite element (HONDOII, HONDOIII, DYNA2D, ANSYS, ABAQUS) and finite difference (PISCES-2DELK, MANJUSRI-2D) types.

2.1 Model A

Model A, shown in Figure 1, represents a steel bar impacting an unyielding target with a velocity of 13.41 m/s (528 ips). This is the simplest problem. It tests the ability of the code to simulate a purely elastic response with an axisymmetric geometry. It is incorporated because it has an approximate analytical solution based on Love's theory (12). The material properties are given in Table I. These are representative of the elastic properties of stainless steel.

Table I: Elastic Steel Properties

Young's Modulus, E	1.9305×10^5 MPa (28×10^6 psi)
Poisson's Ratio, ν	0.3
Density, ρ	8,027 kg/m^3 (0.29 lbm/in^3)

The results required for this problem are: (1) impact duration (milliseconds), T; (2) rebound velocity (m/s); and (3) plot of stress (MPa) versus rod length (m) at T/4.

The impact duration can be determined by one of three methods. These are when (1) the model separates from the rigid target, (2) all velocities in the model become opposite in sign from the initial velocity, or (3) the velocity of the center of gravity becomes opposite in sign from its initial velocity. Each of the methods requires different code or post processing capability.

The rebound velocity should be determined from the center of gravity. This eliminates the natural vibrational modes which would be included in individual node or element responses.

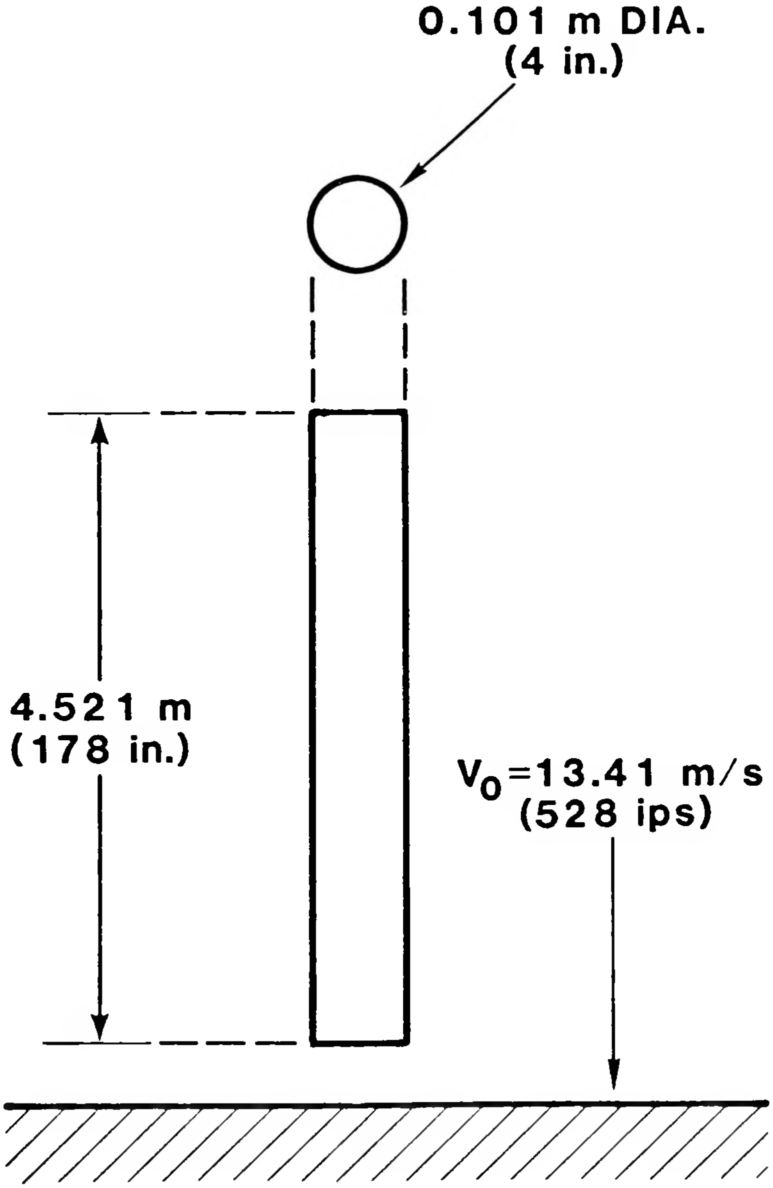

Figure 1. Model A--Elastic Steel Rod

Table II contains the tabular results for this problem.

Table II: Model A--End Impact of an Elastic Rod: Results

	Impact Duration (ms)	Rebound Velocity (m/s)
Mean	1.86	13.3
Standard Deviation	0.02	0.15

Figure 2 shows the axial stress as a function of rod length based on Love's theory and the envelope of the numerical solutions.

2.2 Model B

Model B, shown in Figure 3, consists of an annular cylinder impacting an unyielding target at 13.41 m/s (528 ips). The material properties are given in Table III. This problem tests the ability of the code to simulate the nonlinear behavior associated with plastic deformation in an axisymmetric geometry.

Table III: Elastic/Perfectly Plastic Steel Properties

Young's Modulus, E	1.9305×10^5 (28×10^6 psi)
Poisson's Ratio, ν	0.3
Density, ρ	8,027 kg/m^3 (0.29 lbm/in^3)
Yield Strength, σ_y	206.8 MPa (30,000 psi)

The results required for this problem are: (1) impact duration (milliseconds), (2) rebound velocity (m/s), and (3) final axial deformation (m). The final axial deformation should be determined by time averaging the distance between extreme axial nodes during rebound. This again eliminates the vibrational response of the cylinder.

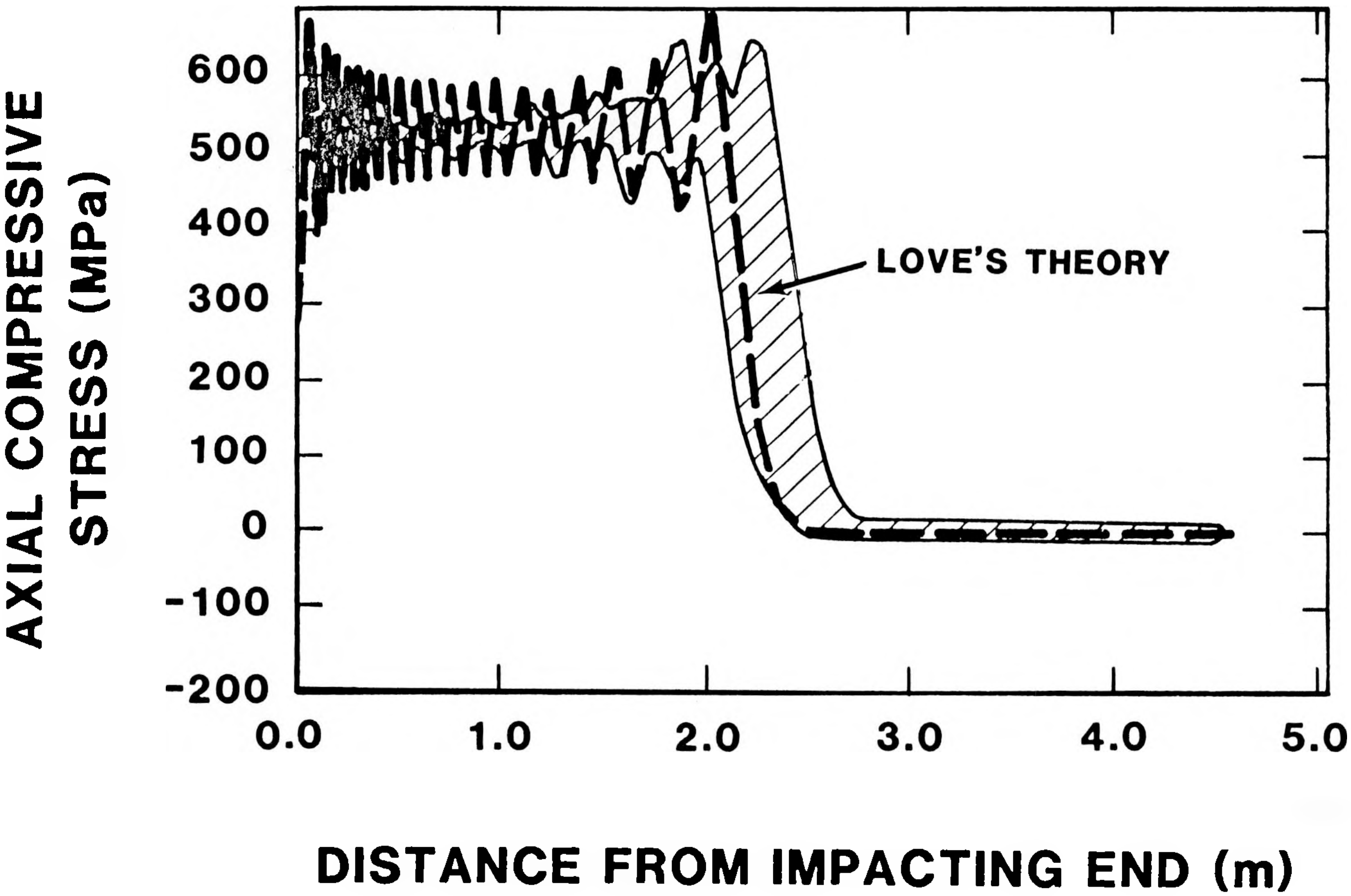

Figure 2. Model A--Axial Stress as a Function of Rod Length at Time, T/4

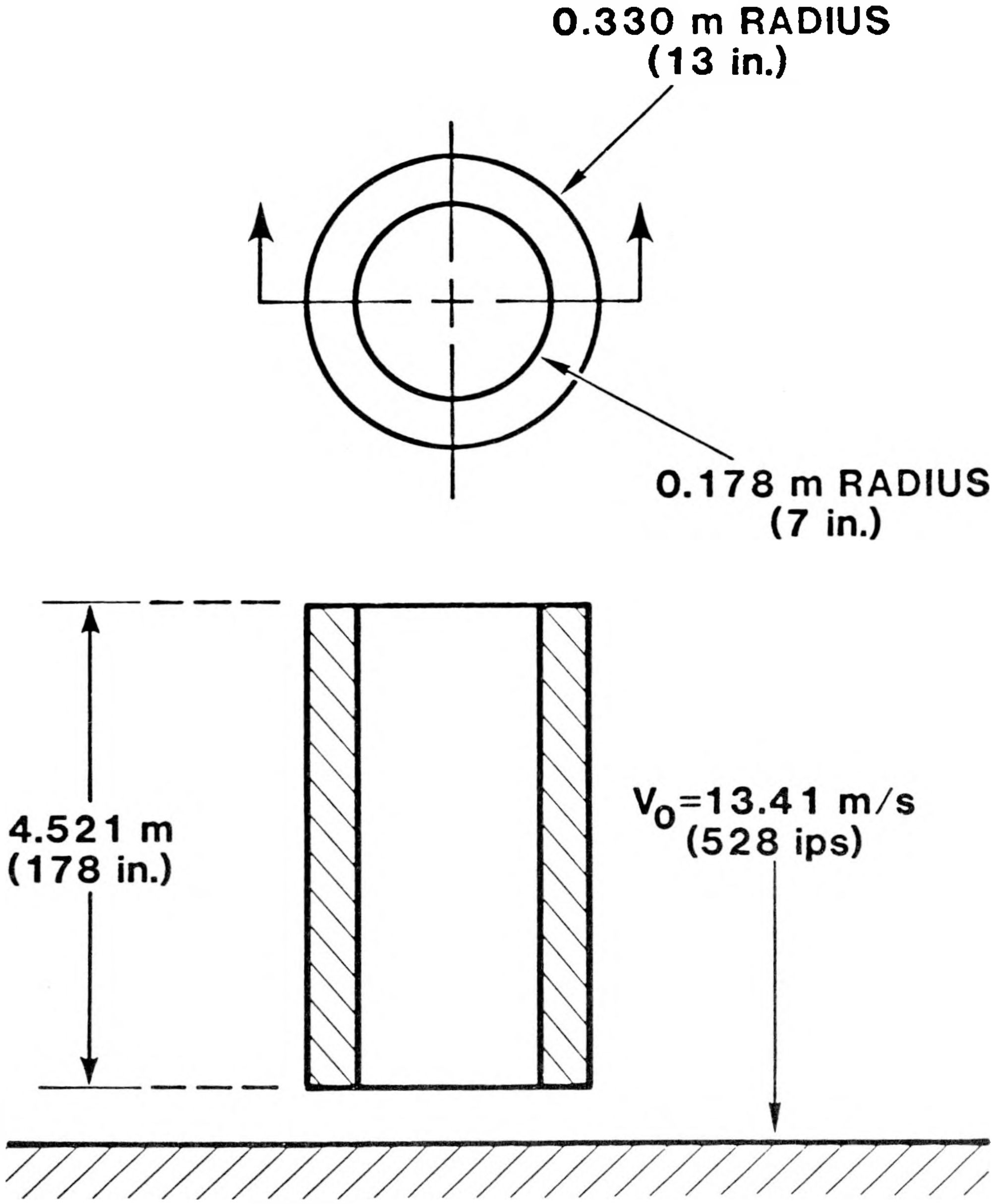

Figure 3. Model B--End Impact of an Elastic/Perfectly Plastic Cylinder

Table IV contains the tabular results for this problem.

Table IV: Model B--End Impact of an Elastic/Perfectly Plastic Rod: Results

	Impact Duration (ms)	Rebound Velocity (m/s)	Final Axial Deformation (m)
Mean	3.46	3.30	0.0146
Standard Deviation	0.27	0.45	0.0008

2.3 Model C

Model C, as shown in Figure 4, represents an annular steel cylinder impacting an unyielding target at 13.41 m/s (528 ips). The material properties are given in Table I. Plane strain is assumed. This problem tests the code's ability to predict elastic response for a plane strain problem typical of side impacts. The required results are: (1) impact duration (ms), (2) rebound-velocity (m/s), and (3) the horizontal stress (MPa) versus time (ms) at the inside radius impact point.

Table V contains the tabular results for this problem.

Table V: Model C--Side Impact of an Annular Elastic Steel Cylinder: Results

	Impact Duration (ms)	Rebound Velocity (ms)
Mean	0.78	13.1
Standard Deviation	0.038	0.23

Figure 5 shows an envelope of the horizontal stress as a function of time for the inner radius of the cylinder at the impact point.

2.4 Model D

Model D, as shown in Figure 6, simulates an annular steel cylinder impacting an unyielding target of 13.41 m/s (528 ips). It provides a direct measure of the effect of plasticity. The geometry and initial conditions duplicate Model C with the substitution of the elastic/plastic material

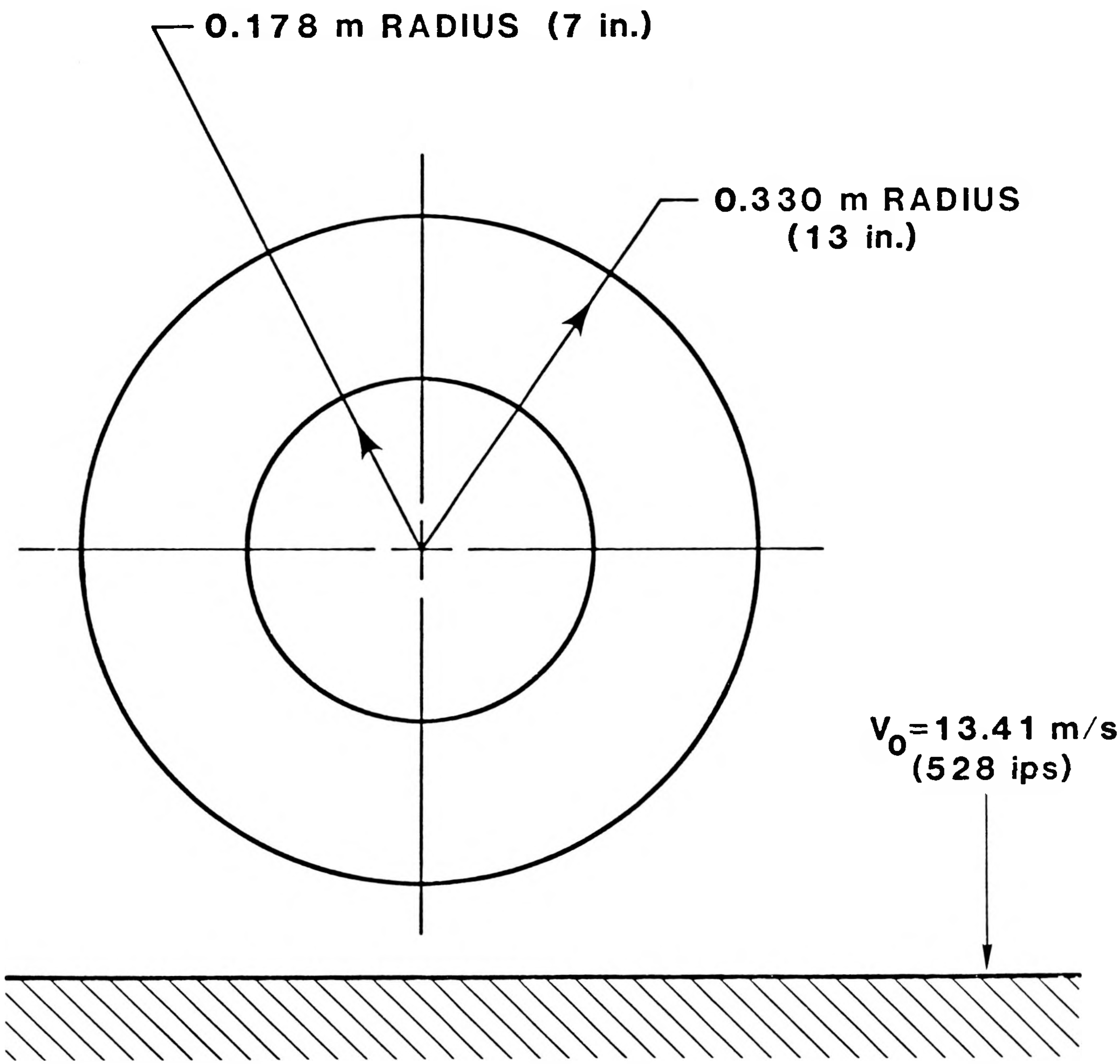

Figure 4. Model C--Side Impact of an Annular Elastic Steel Cylinder

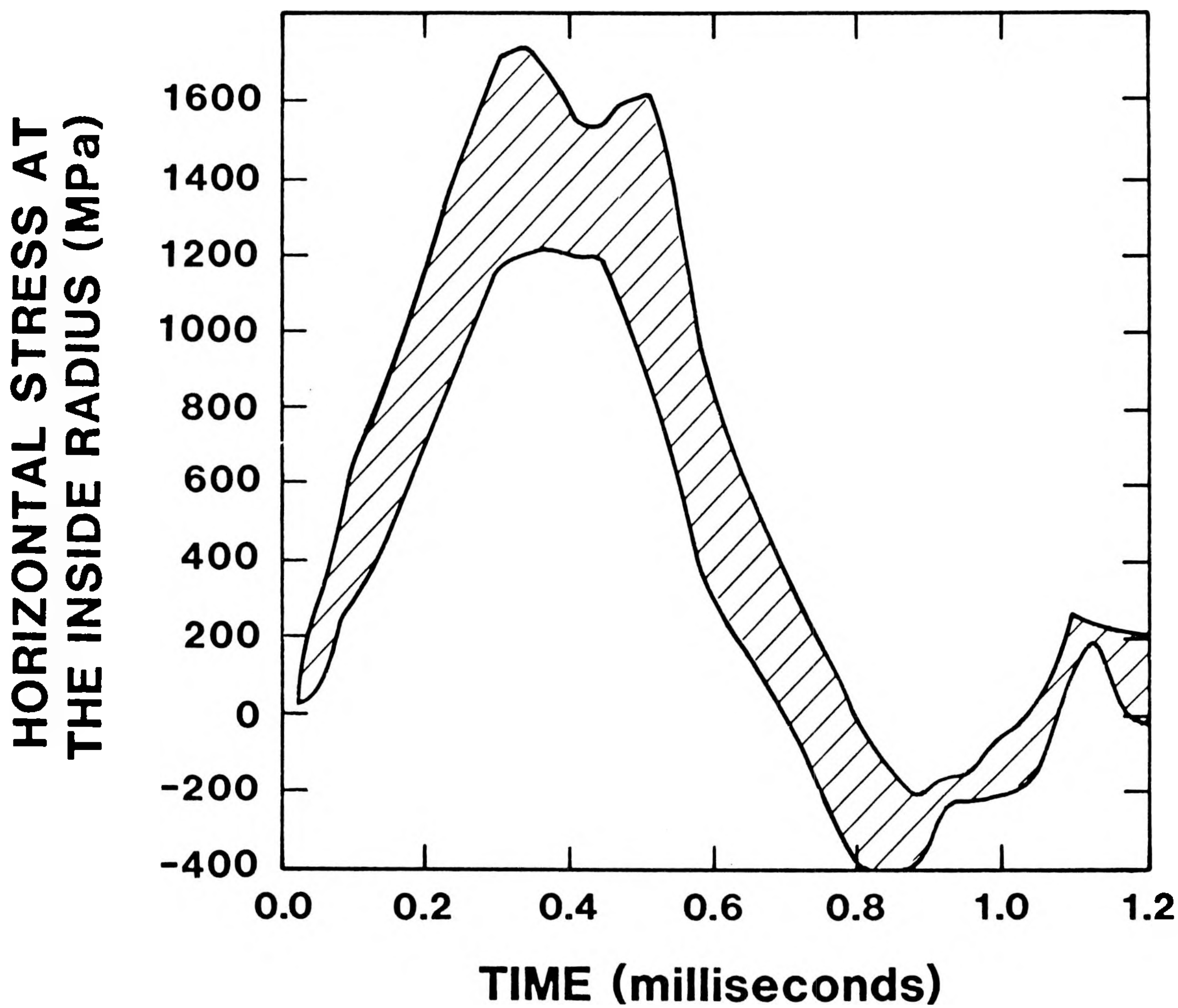

Figure 5. Model C--Horizontal Stress as a Function of Time

properties given in Table III. The requested results are: (1) impact duration (ms), (2) rebound velocity (m/s), (3) permanent horizontal ovalization (%), and (4) permanent vertical ovalization (%).

The permanent ovalizations are determined by the ratio of the change in outside diameter to the original diameter. Again, the vibrational response of the model requires that averaged differences between opposing nodes should be used instead of single time values.

Table VI contains the tabular results for this problem.

Table VI: Model D--Side Impact of an Annular Elastic/ Perfectly Plastic Steel Cylinder: Results

	Impact Duration (ms)	Rebound Velocity (m/s)	Horizontal Ovalization (%)	Vertical Ovalization (%)
Mean	1.15	3.43	0.29	0.88
Standard Deviation	0.11	0.40	0.063	0.12

2.5 Model E

Model E, as shown in Figure 7, simulates a steel clad lead cylinder. The lead and steel are attached at the impacting end. The cylinder impacts an unyielding target with an initial velocity of 13.41 m/s (528 ips). The steel/lead interface should be treated as frictionless. The steel properties are given in Table III, and the lead properties are given in Table VII. This problem will test both interface capability and the simulation of much greater plasticity. This is reflected in the lower rebound velocity.

Table VII: Elastic/Perfectly Plastic Lead Properties

Young's Modulus, E	1.3789×10^4 MPA	(2×10^6 psi)
Poisson's Ratio, ν	0.45	
Density, ρ	1.135×10^4 kg/m^3	(0.41 lbm/in^3)
Yield Strength, σ_y	13.78 MPa	(2,000 psi)

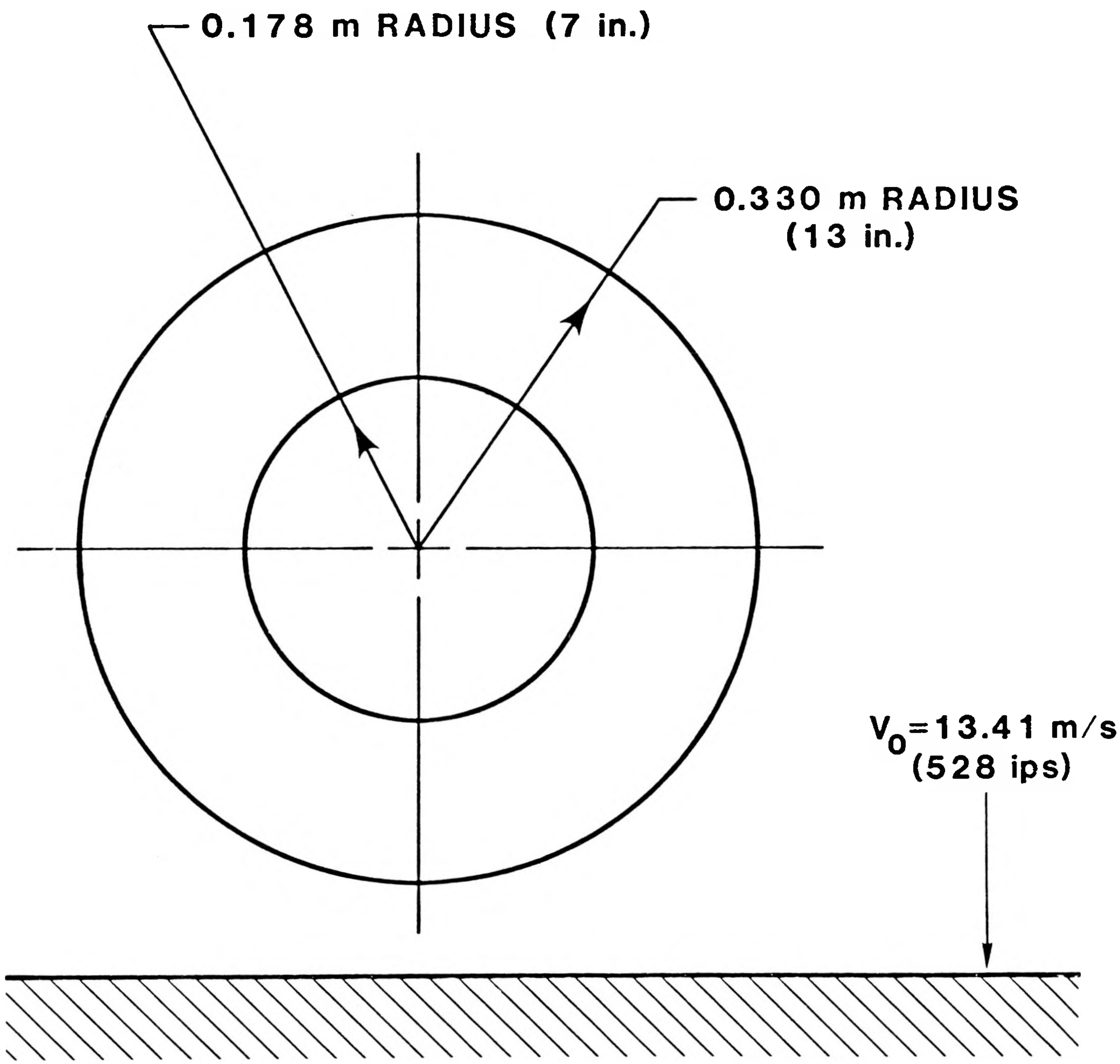

Figure 6. Model D--Side Impact of an Annular Elastic/Perfectly Plastic Steel Cylinder

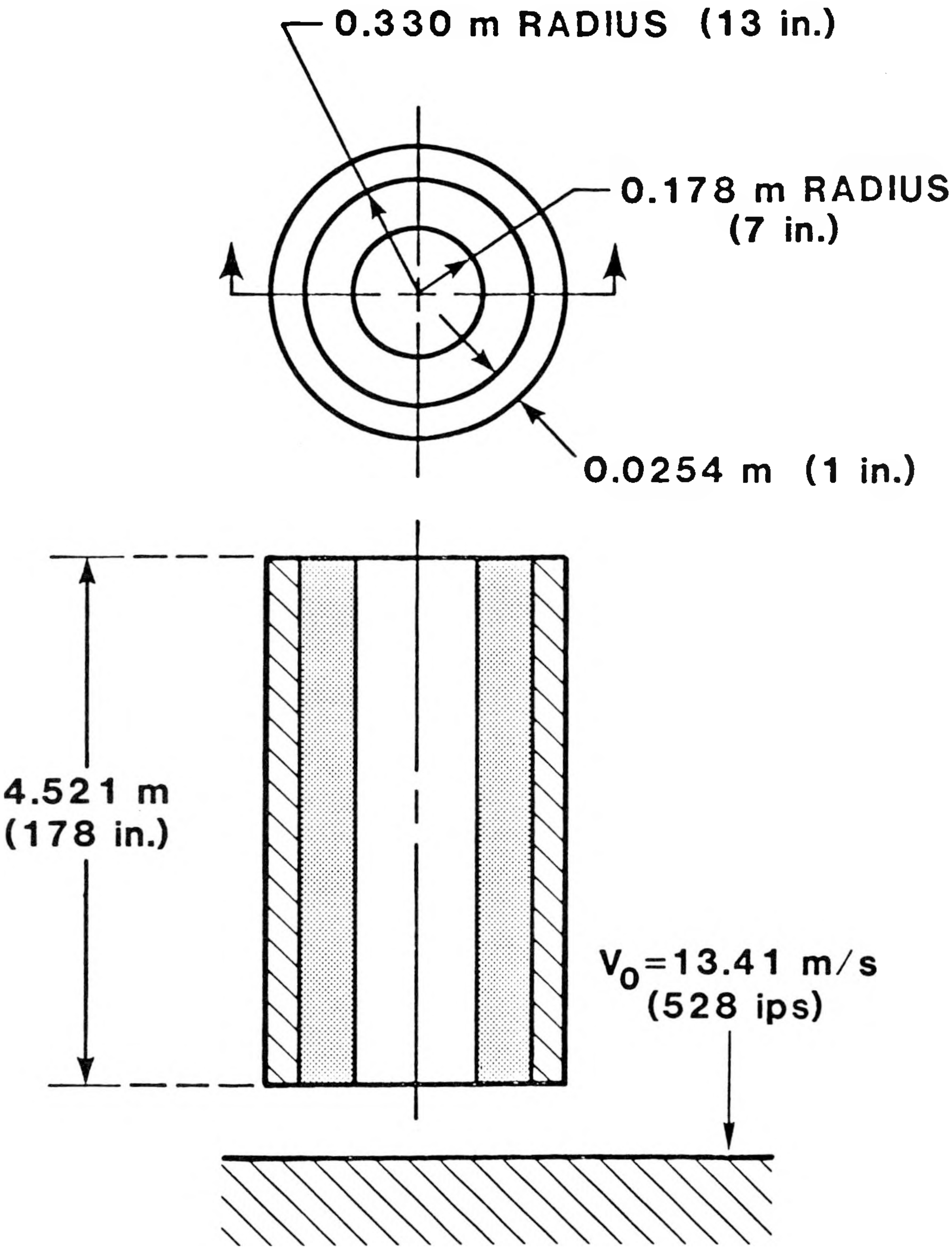

Figure 7. Model E--End Impact of an Elastic/Perfectly Plastic, Steel-Clad Annular Lead Cylinder

The results required for this problem are: (1) the impact duration (ms), (2) average lead rebound velocity (m/s), (3) final lead axial deformation (m), and (4) final steel cladding deformation (m). Each deformation is determined by time averaging the distance between extreme axial nodes during rebound.

Table VIII contains the tabular results for this problem.

Table VIII: Model E--End Impact of an Elastic/Perfectly Plastic Steel Clad Annular Lead Cylinder: Results

	Impact Duration (ms)	Lead Rebound Velocity (m/s)	Axial Lead Deformation (m)	Axial Steel Deformation (m)
Mean	29.0	0.83	0.18	0.022
Standard Deviation	3.01	0.028	0.036	0.000

3.0 Thermal Problems

The thermal problems simulate normal transport and accident conditions specified in 10CFR71. The regulations define a thermal event as "exposure of the whole specimen for not less than 30 minutes to a heat flux not less than that of a radiation environment of 800°C (1475°F) with an emissivity coefficient of at least 0.9. For purposes of calculation, the surface absorptivity must be either that value which the package may be expected to possess if exposed to a fire or 0.8, whichever is greater."

To completely model the thermal event requires simulating conduction, convection, and radiation. The problems included in this manual will exercise these facets of a code. There are additional phenomena that are not included in this problem set, such as phase change (lead melt) and boiling water heat transfer.

The codes whose results are used here were COYOTE (13), HEATING-5 (14), Q/TRAN (15), TAC-2D (16), TEMPEST (17), and TRUMP (18). Subsequently, HEATING-6 (19), DELFINE, and TAU have been used. These additional codes' results agreed with the initial results.

3.1 Model A

Model A, shown in Figure 8, is a two-region cylinder. The interior region (Region I) contains a volumetric heat source representative of the internal decay heat of irradiated fuel. This energy is dissipated at the outer surface by convection. This problem, which has a closed form analytical solution, tests the ability of the codes to simulate conduction and a convective boundary condition.

The geometric and thermal characteristics are given in Table IX.

Table IX: Model A--Cylinder with Internal Heat Generation: Characteristics

	Region I	Region II
Radius, r	r_1 = 27.43 cm (10.8 in.)	r_2 = 91.44 cm (36 in.)
Length, L	457.2 cm (15 ft.)	457.2 cm (15 ft.)
Density, ρ	16.02 kg/m^3 (1 lbm/ft^3)	16.02 kg/m^3 (1 lbm/ft^3)
Specific Heat, C	1 cal/gm - °C (1 Btu/lbm°F)	1 cal/gm °C (1 Btu/lbm°F)
Conductivity, k	0.0692 kw/m°C (40 Btu/hr ft °F)	0.0346 kw/m°C (20 Btu/hr ft °F)
Heat Source, Q	11.09 kw/m^3 (1071.5 Btu/hr ft^3)	--
Convective Coefficient, h	--	5.67×10^{-3} kw/m^2°C (1 Btu/hr ft^2 °F)

The ambient environment and initial cask temperature are each 54.4°C (130°F).

The steady state results requested for this problem are: (1) centerline temperature, (2) interface temperature (r_1), (3) outer edge temperature, and (4) plot of temperature versus normalized radial position.

The closed form analytical and numerical solutions reported to 1° accuracy are given in Table X, and the graphical solution reported to 0.1° accuracy in Figure 9.

Table X: Model A--Cylinder with Internal Heat Source: Results

	Centerline (°C)	Interface (°C)	Outer Edge (°C)
Exact (closed form)	152	149	135
Mean	152	149	135

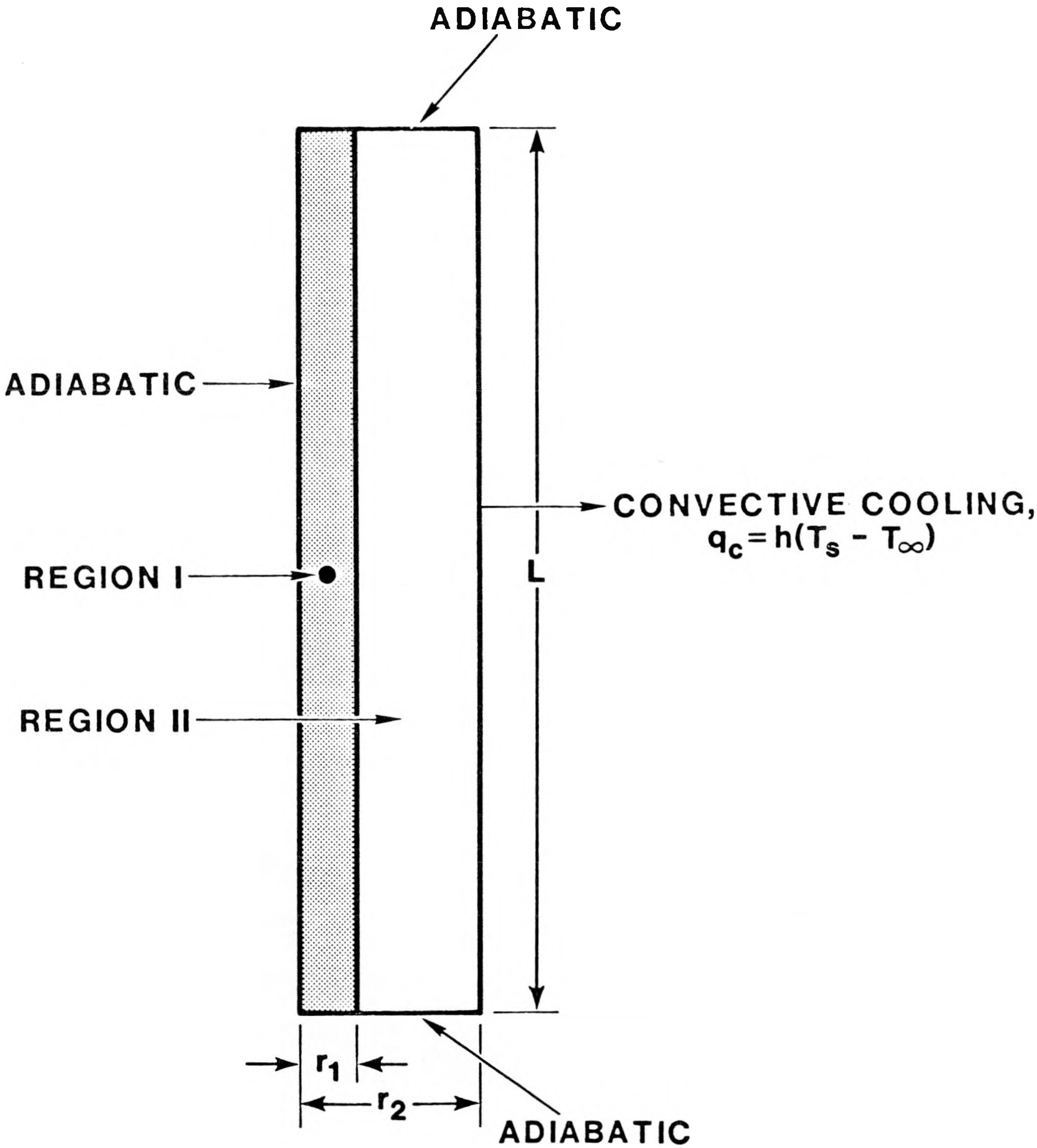

Figure 8. Model A--Cylinder with Internal Heat Generation

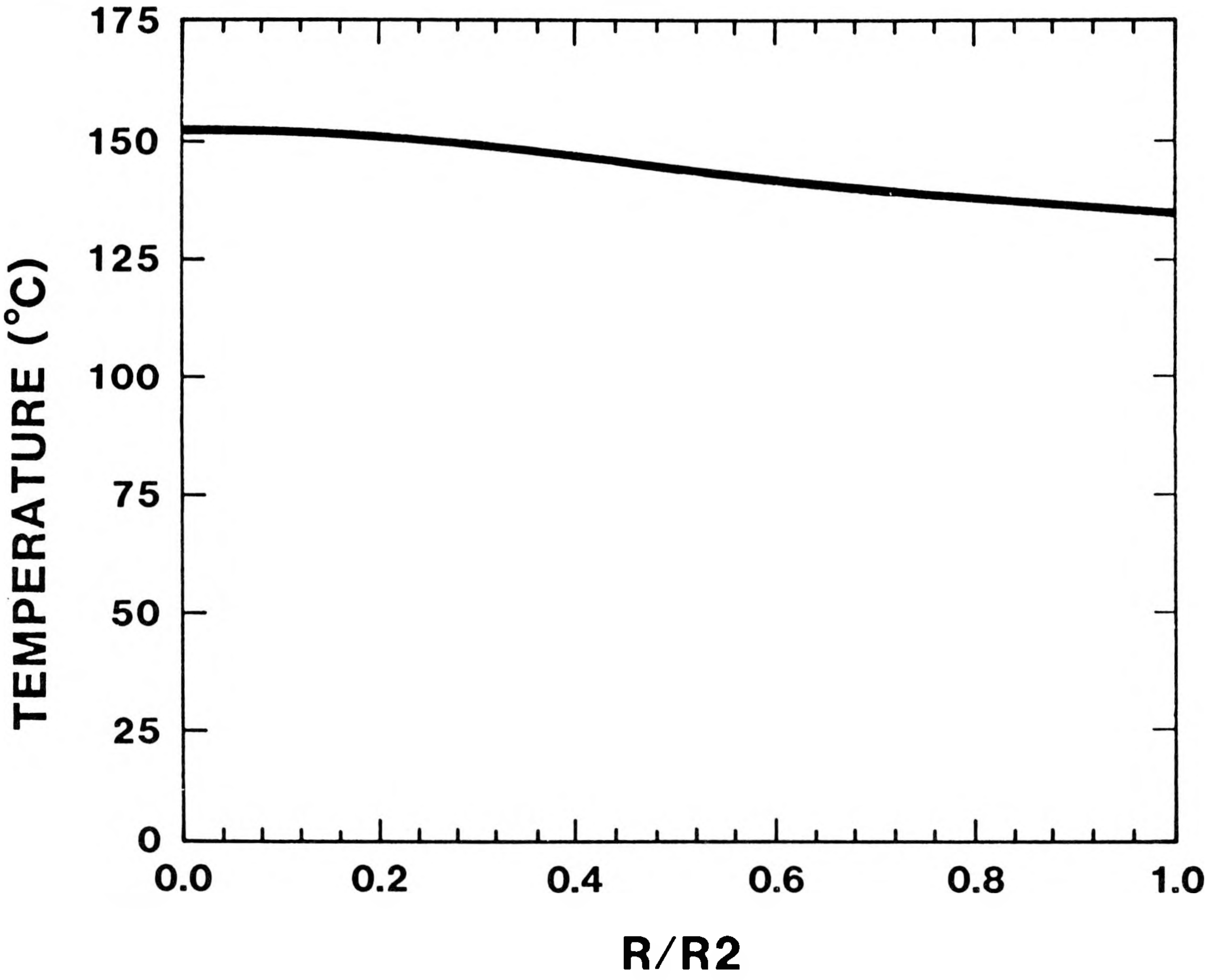

Figure 9. Modél A--Temperature Versus Normalized Radial Position

3.2 Model B

Model B, shown in Figure 10, is based on a prototypic cask configuration consisting of several different annular regions. Region I contains a volumetric heat source simulating irradiated fuel decay heat. Region II represents a monolithic cask wall. Region III is a voided neutron shield, and Region IV the thermal radiation shield. Regions II and IV exchange heat solely by thermal radiation. Heat is also exchanged with the surrounding environment by thermal radiation. For simplicity, all surfaces and the environment are assumed black ($\epsilon = \alpha = 1$).

This problem simulates exposure to the regulatory fire. This involves three regimes. First, a steady state solution, with radiant heat loss to a 54.4°C (130°F) environment, is required. Second, using the steady state solution for the initial conditions, the fire is simulated by a step increase of the ambient temperature to 800°C (1475°F) for 30 minutes. A cool down period of 60 minutes follows the fire with the ambient temperature returned to 54.4°C (130°F). In each case, heat transfer between the cask and the environment is solely by black body radiation.

The geometric and thermal characteristics for Model B are given in Table XI.

Table XI: Model B--Cask with Annular Regions: Characteristics

	Region I	Region II	Region III	Region IV
Radius, r	16.51 cm (6.9 in)	38.74 cm (15.25 in)	53.98 cm (21.25 in)	54.61 cm (21.5 in)
Density, ρ	2707 kg/m^3 (169 lbm/ft^3)	7832.8 kg/m^3 (489 lbm/ft^3)	--	7832 kg/m^3 (489 lbm/ft^3
Specific Heat, C_p	0.214 cal/gm - °C (0.214 Btu/lbm°F)	0.113 cal/gm°C (0.113 Btu/lbm°F)	--	0.113 cal/gm°C (0.113 Btu/lbm°F
Conductivity, k	0.242 kw/m°C (139.7 Btu/hr ft°F)	0.045 kw/m°C (26 Btu/hr ft°F)	--	0.045kw/m°C 26 Btu/hr ft °F)
Heat Source, Q	38.32 kw/m^3 (3702.6 Btu/hr ft^3)	--	--	--

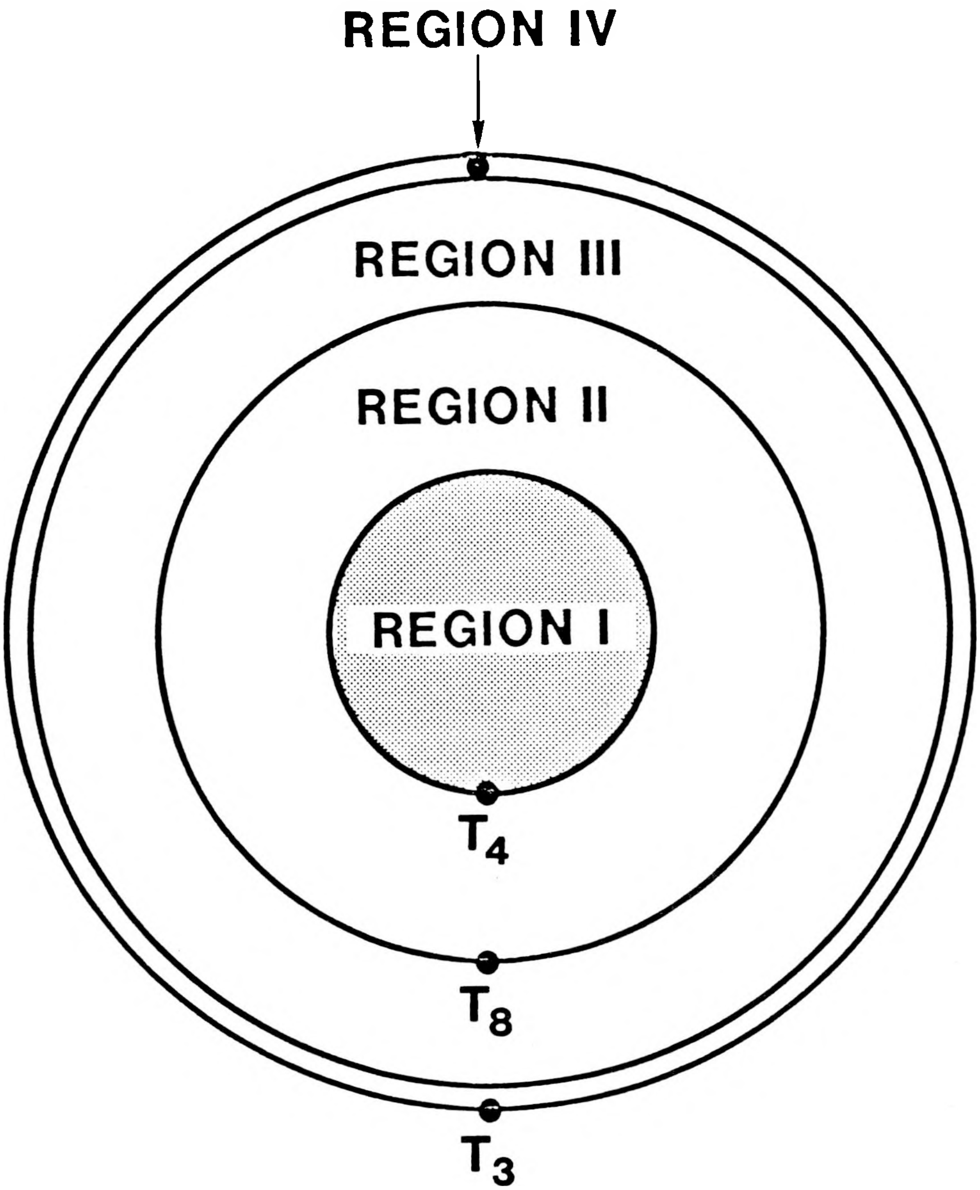

Figure 10. Model B--Cask with Annular Regions

The results requested for this problem are temperatures at: (1) the exterior surface, T3; (2) the interface between Region II and Region III, T8; and (3) the interface between Region I and Region II, T4, as shown in Figure 10. The temperatures are requested in tabular form within 1°C accuracy at 0, 30, and 90 minutes and in graphical form with temperature versus time. The tabular results are given in Table XII, and the graphical results in Figures 11 through 13. The greatest temperature deviation from the mean in the tabular data was 6°C at the interface between Region II and Region III at 90 minutes.

Table XII: Model B--Cask with Annular Regions: Results

Time (Minutes)	T3 (°C)	T8 (°C)	T4 (°C)
0	137	204	214
30	689	376	263
90	203	298	313

3.3 Model C

Model C is a modification of Model B. A flat plate has been added as shown in Figure 14. This plate simulates a truck bed which acts as a thermal shield. The addition of this plate forces the code to simulate a two-dimensional thermal radiation problem. Radiant heat transfer occurs between the cask and the ambient and also between the cask and the shield. The remainder of the problem is as described for Model B. The properties of the shield are given in Table XIII.

Table XIII: Model C--Shield Characteristics

Width, W	109.2 cm (43 in.)
Thickness, δ	2.54 cm (1 in.)
Distance from Cask, D	30.48 cm (12 in.)
Density, ρ	7832.8 kg/m^3 (489 lbm/ft^3)
Specific Heat, C_p	0.113 cal/gm°C (0.113 Btu/lbm°F)
Conductivity, k	0.045 kw/m°C (26 Btu/hr ft°F)

The results requested are tabular data at: (1) the center of the shield exposed to the environment, T1; (2) the cask exterior facing the shield center, T3; (3) the interface between Region II and Region III, T8; (4) the interface between Region I and Region II, T4; and (5) the exterior of the reg7045

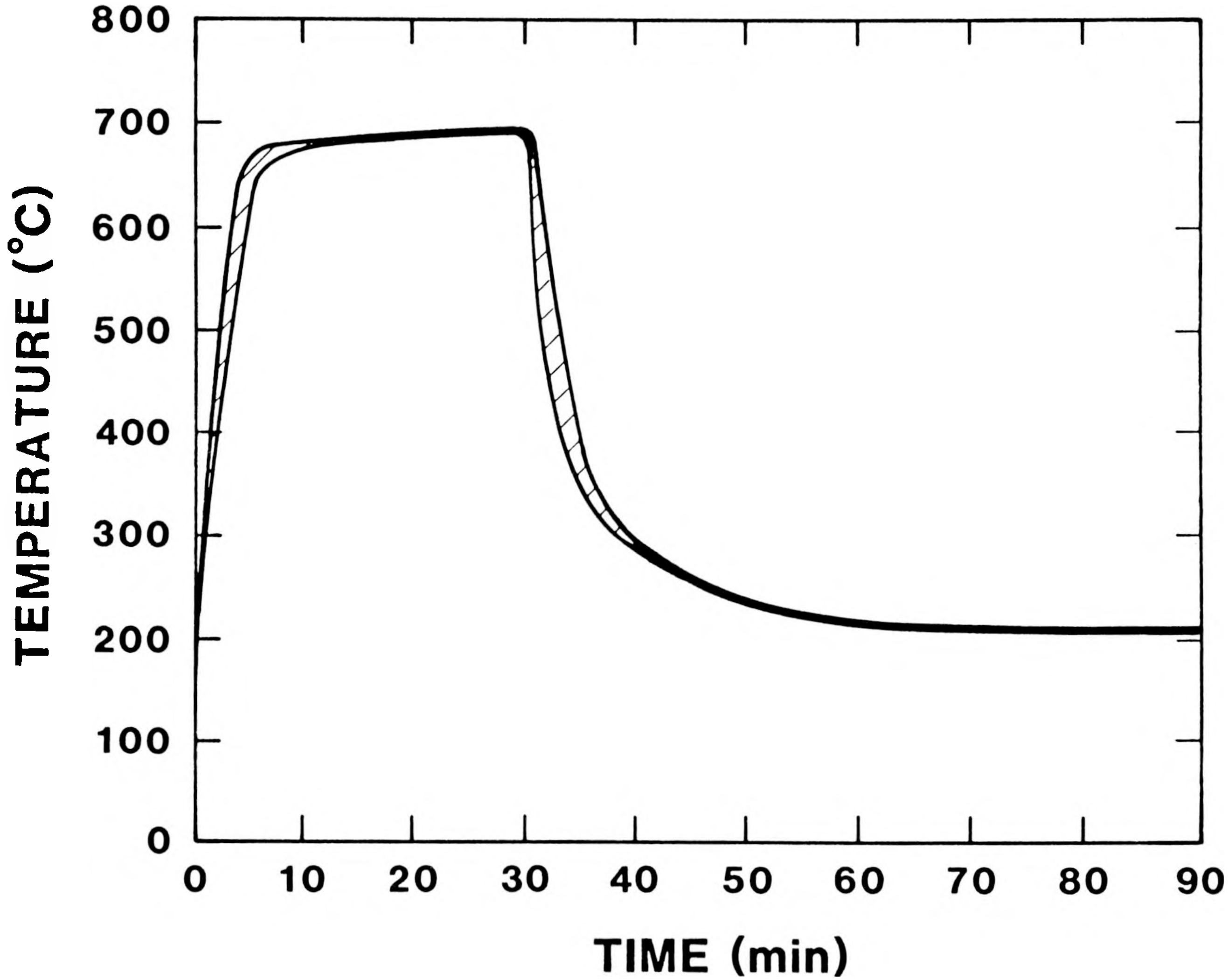

Figure 11. Model B--Temperature Versus Time at Cask Surface

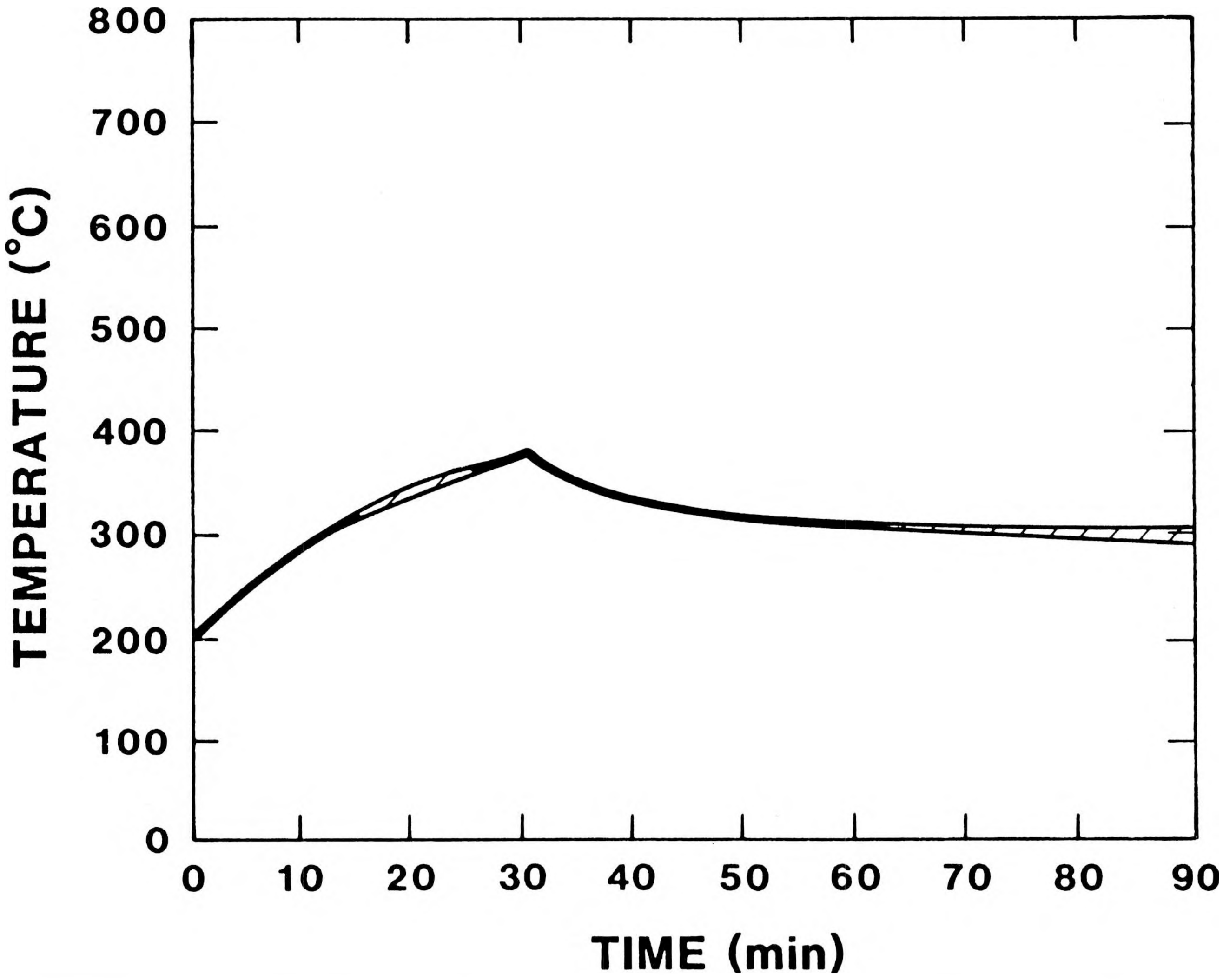

Figure 12. Model B--Temperature Versus Time at Interface Between Region II and Region III

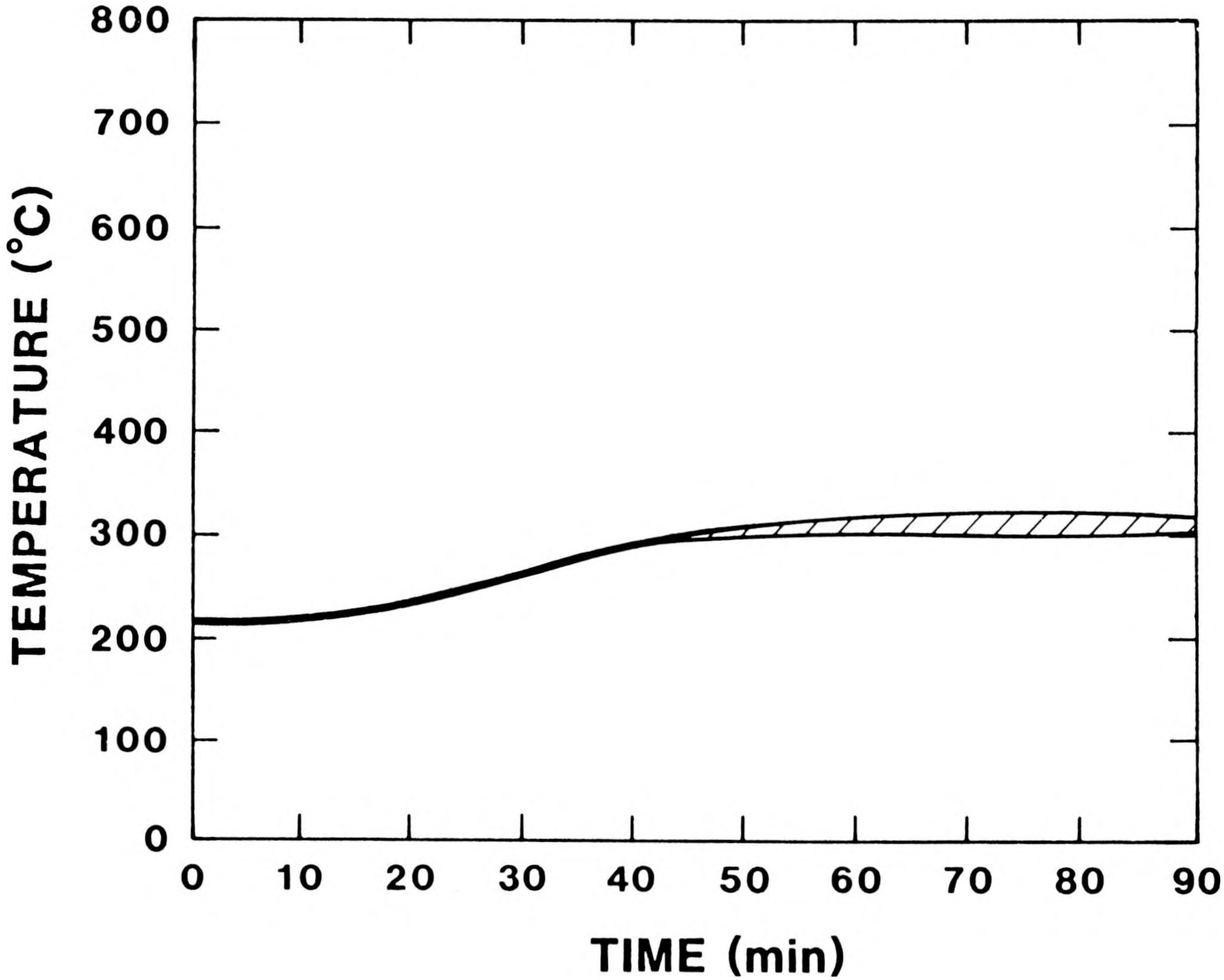

Figure 13. Model B--Temperature Versus Time at Interface Between Region I and Region II

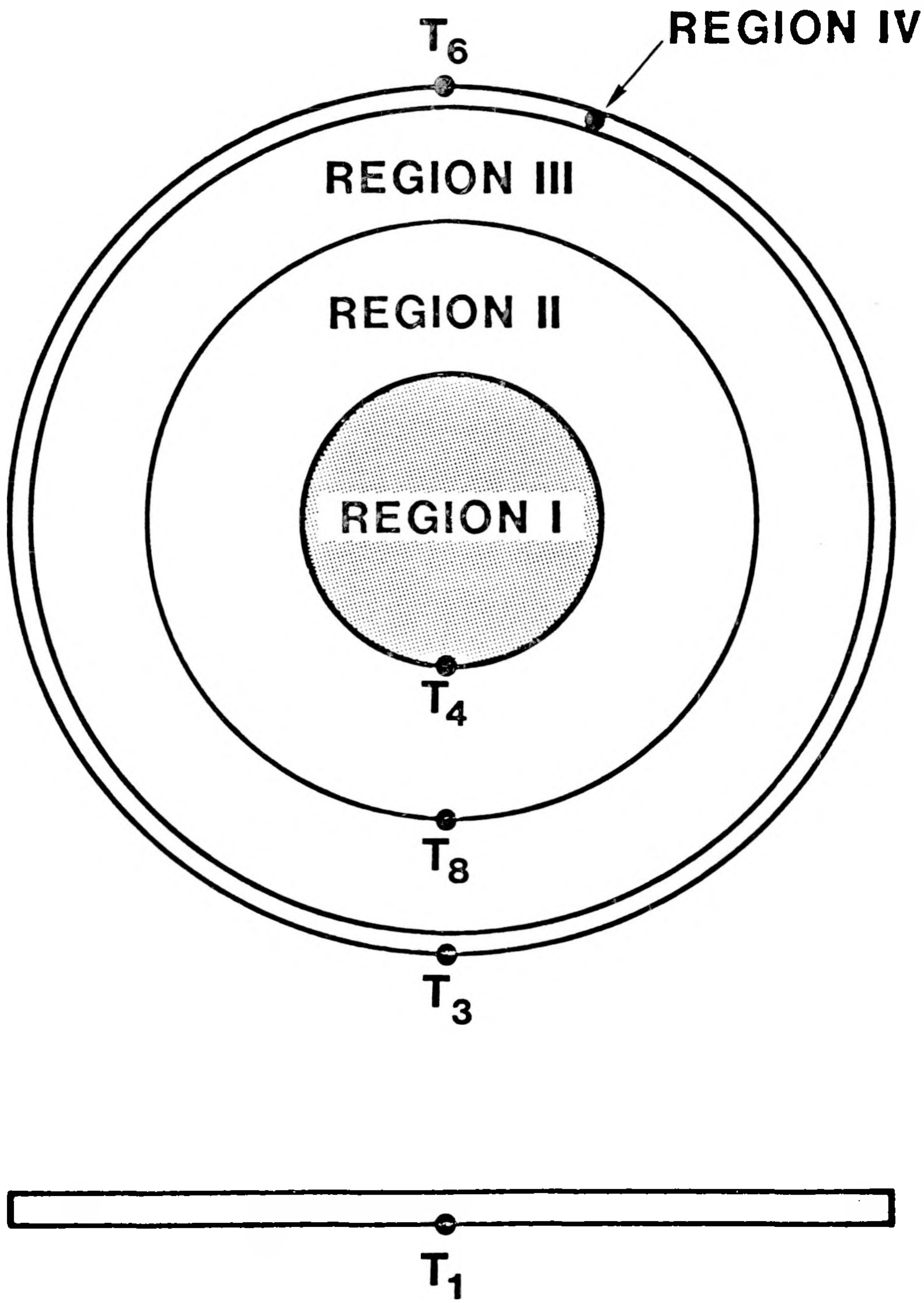

Figure 14. Model C--Cask with Annular Regions and Shield

cask, T6, as shown in Figure 14. This data is requested at 0, 30, and 90 minutes. The graphical data requested are temperature versus time plots at these locations. Three of the original codes solve explicit two-dimensional thermal radiation problems. These are CINDA-3G, Q/TRAN, and TAC-2D. The tabular results given in Table XIV and the graphical results in Figures 15 through 19 represent only these three codes.

Table XIV: Model C--Cask with Annular Regions and Shield: Results

Time (Minutes)	T1 (°C)	T3 (°C)	T4 (°C)	T6 (°C)	T8 (°C)
0	89	147	217	139	208
30	765	662	261	689	350
90	206	245	314	203	301

The largest deviation from the mean temperatures was 4°C at Location T4 after 30 minutes.

4.0 Conclusion

This report contains structural and thermal problems and the corresponding numerical solutions. These solutions were obtained from several codes and code types. These results can be used in evaluating codes being used in the design and certification of radioactive materials packagings. They can also be used by analysts as a check on code usage including choice of mesh size, time step, and materials model.

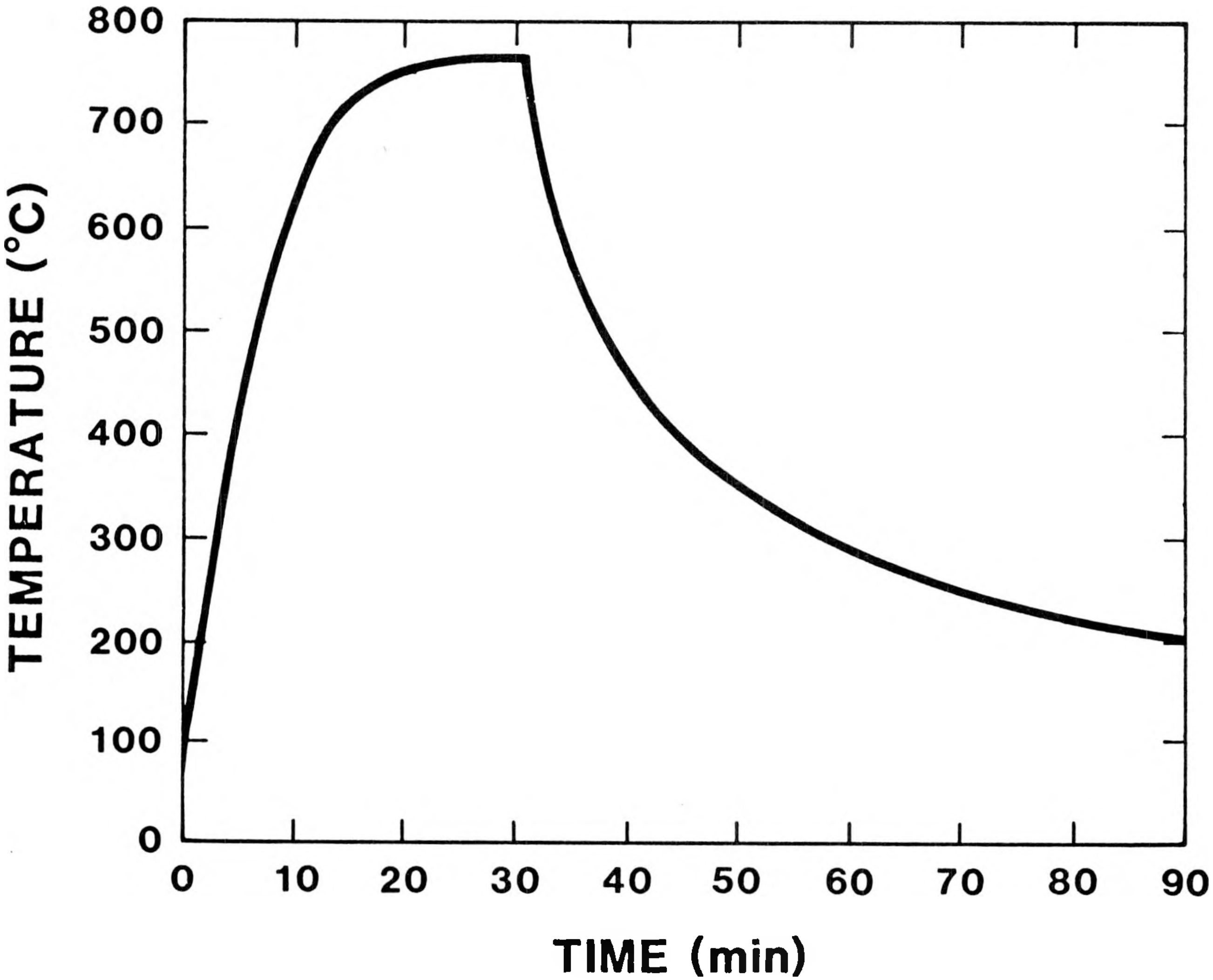

Figure 15. Model C--Temperature Versus Time on Shield

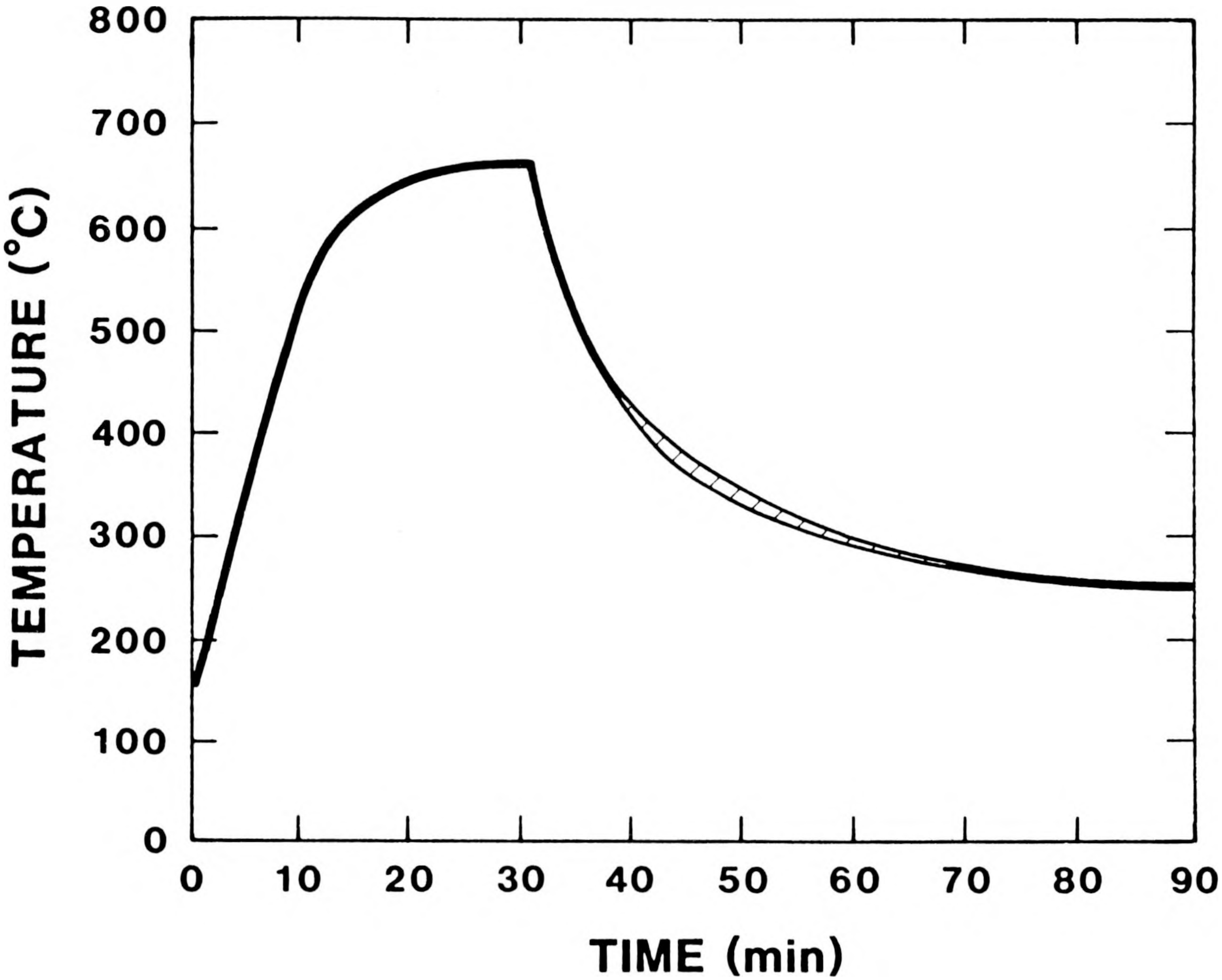

Figure 16. Model C--Temperature Versus Time at Cask Surface Facing Shield

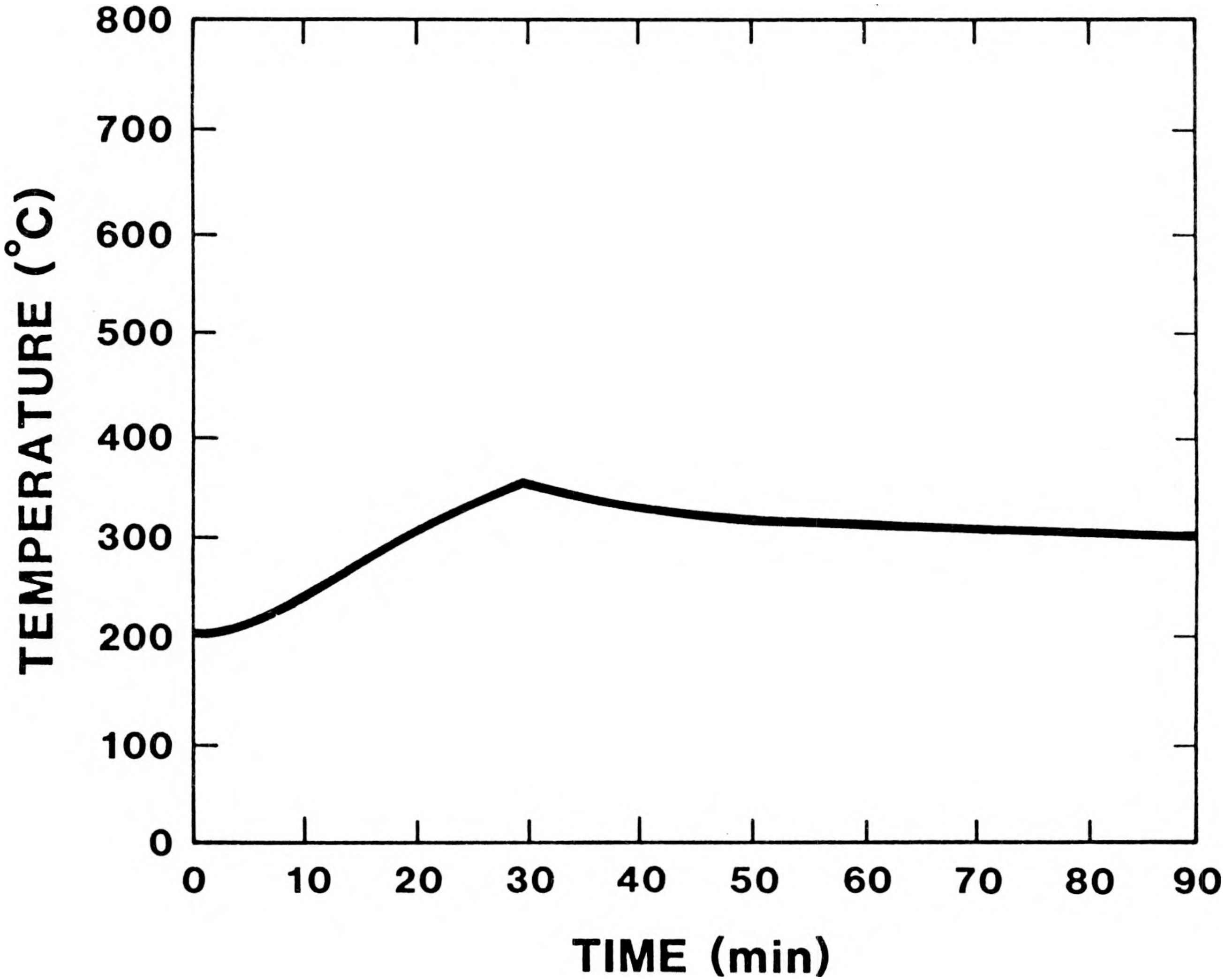

Figure 17. Model C--Temperature Versus Time at Voided Region Interface

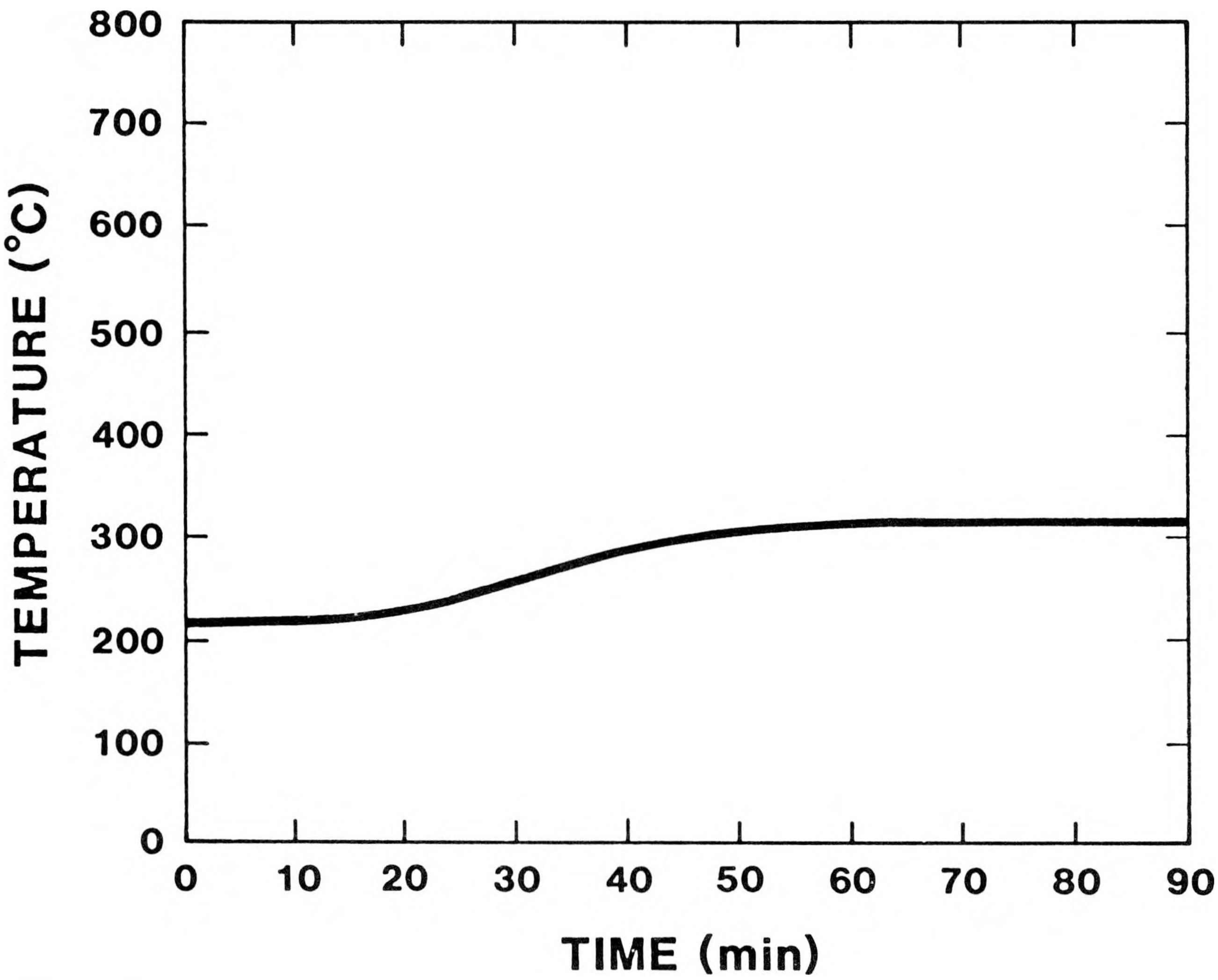

Figure 18. Model C--Temperature Versus Time at Heat Generation Region Interface

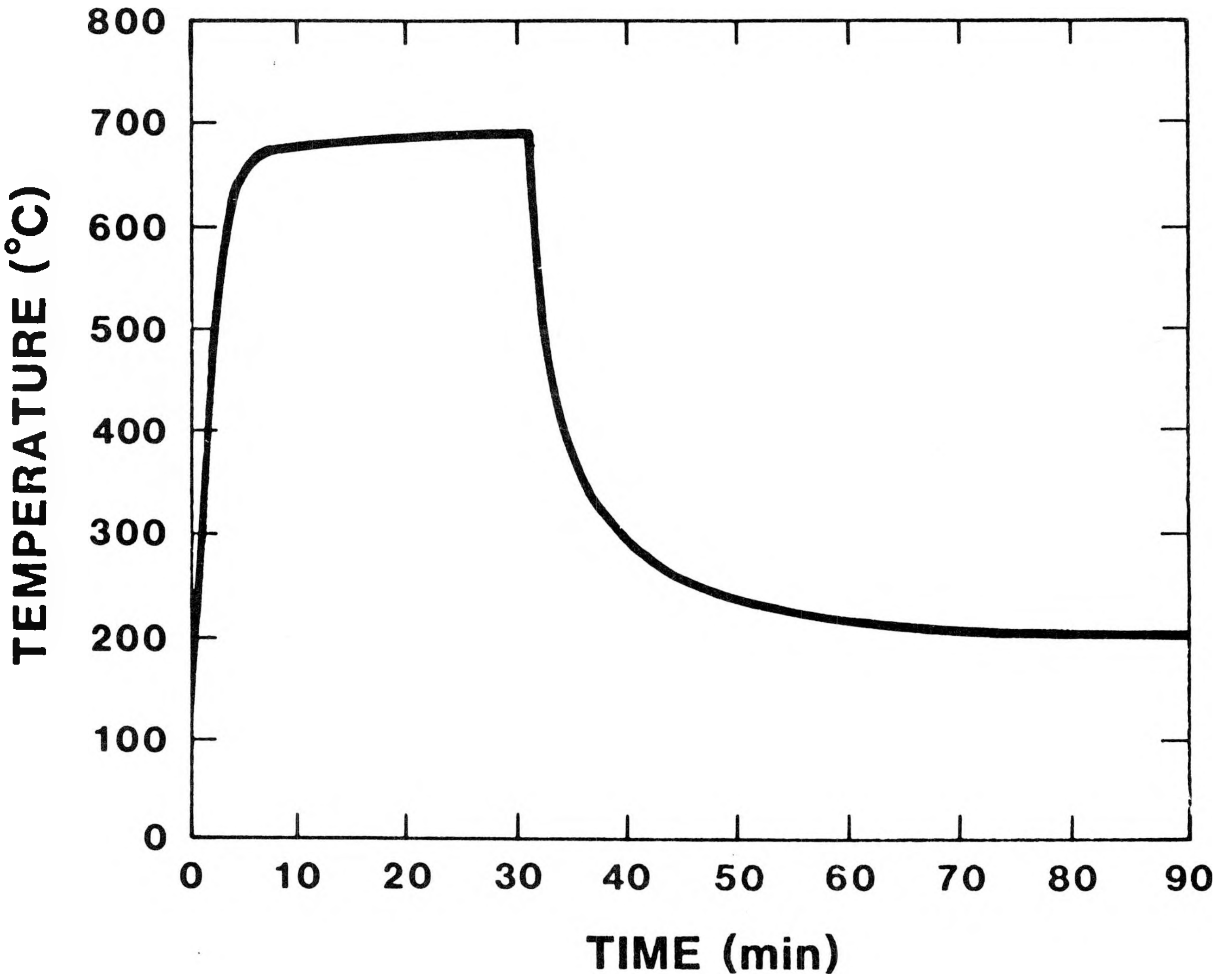

Figure 19. Model C--Temperature Versus Time at Cask Surface Exposed to Environment

REFERENCES

(1) OECD Nuclear Energy Agency, Committee on the Safety of Nuclear Installations, Standard Problem Exercise on Criticality Codes for Large Arrays of Packages of Fissile Materials, Paris, France, August 1984.

(2) Glass, R. E., et al. "Standard Thermal Problem Set for the Evaluation of Heat Transfer Codes Used in the Assessment of Transportation Packages," presented at the 30th Annual Nuclear Energy Agency Committee on Reactor Physics Meeting, Helsinki, Finland, September, 1987.

(3) Nelsen, J. M. (ed.) "Industry/Government Joint Thermal and Structural Codes Information Exchange Meeting," TTC-0404, Sandia National Laboratories, Albuquerque, New Mexico, October 1982.

(4) Glass, R. E. "Structural Code Benchmarking for the Analysis of Impact Response of Nuclear Materials Shipping Casks," SAND84-1855, Sandia National Laboratories, Albuquerque, New Mexico, March 1985.

(5) Glass, R. E., et al., "Structural Code Benchmarking: Impact Response Resulting from the Regulatory 9-Meter Drop," Proceedings of the Symposium on Waste Management, Volume 3, March 1985.

(6) Sanchez, L. C. (ed.), "Performance Testing of Thermal Analysis Codes for Nuclear Fuel Casks," SAND84-1854, Sandia National Laboratories, Albuquerque, New Mexico, January 1987.

(7) Key, S. W., Z. E. Beisinger, and R. D. Krieg. HONDO-II A Finite Element Computer Program for the Large Deformation Dynamics Response of Axusymmetric Solids, SAND78-0422, Sandia National Laboratories, Albuquerque, NM, November, 1978.

(8) Key, S. W. HONDO-III Theoretical and User's Manual, RSICAL01-0194, REISPEC, Inc., Albuquerque, NM, May 1987.

(9) DeSalvo, G. J., and J. A. Swanson. ANSYS Engineering Analysis System User's Manual, Rev. 3, Swanson Analysis Systems, Houston, PA.

(10) ABAQUS User's Manual, Version 4, July 1982, Hibbitt, Karlsson, and Sorensen, Inc.

(11) Hallquist, J. O. DYNA2D, An Explicit Finite Element and Finite Difference Code for Analyzing Axisymmetric and Plane Strain Calculations, UCRL-52429.

(12) Love, A. E. H. A Treatise on the Mathematical Theory of Elasticity, 4th ed. Dover, 1927.

(13) Gartling, D. K. COYOTE, A Finite Element Computer Program for Nonlinear Heat Conduction Problems, SAND77-1332, June 1978, Sandia National Laboratories, Albuquerque, NM.

(14) Turner, W. D., D. C. Elrod, and I. I. Siman-Tov. HEATING-5, An IBM-360 Heat Conduction Program, ORNL/CSD/TM-15, Oak Ridge National Laboratory, Oak Ridge, TN, 1977.

(15) Rockenbach, F. A. Q/TRAN Version 1.0 User's Manual, The Rock, Inc., Los Alamos, NM, October 1984.

(16) Boonstra, R. H. TAC-2D, A General Purpose Two-Dimensional Heat Transfer Computer Code--User's Manual, GA-A 14032, GA Technologies, July 1979.

(17) Trent, D. S., M. J. Budden, and L. L. Eyler, TEMPEST, A Three-Dimensional Time-Dependent Computer Program for Hydrothermal Analysis, Battelle, Pacific Northwest Laboratory, PNL-5213, July 1984.

(18) Edwards, A. L. TRUMP, A Computer Program for Transient and Steady-State Temperature Distributions in Multidimensional Systems, UCRL-14754, Rev. 2, Lawrence Radiation Laboratory, July 1969 (errata February 1971).

(19) Elrod, D. C., et al. HEATING6: A Multidimensional Heat Conduction Analysis with the Finite-Difference Formulation, ORNL/NUREG/CSD-2/V2, Union Carbide Corporation, Oak Ridge, TN, October 1981.

DISTRIBUTION

No. of Copies	
226	U.S. Department of Energy Office of Scientific & Technical Information Oak Ridge, TN 37830 Attn: DOE/OSTI-4500-R74 UC-71
6	U.S. Department of Energy Routing RW-33 1000 Independence Ave., SW Washington, DC 20585 Attn: L. Barrett G. Callaghan S. Denny W. Lake L. Marks E. Wilmot
2	U.S. Department of Energy Routing RW-32 1000 Independence Ave., SW Washington, DC 20585 Attn: K. Klein D. Shelor
1	U.S. Department of Energy Naval Reactors Routing NE-60 Washington, DC 20585 Attn: R. Kulbitskas
3	U.S. Department of Energy Routing DP-123 Washington, DC 20545 Attn: T. Hindman F. Falci L. Harmon
1	Office of Security Evaluations Defense Programs - DP-4, GTN Washington, DC 20545 Attn: C. Mauck

No. of Copies	
2	U.S. Department of Energy Albuquerque Operations Office Albuquerque Headquarters P.O. Box 5400 Albuquerque, NM 87115 Attn: J. E. Bickel K. G. Golliher
5	U.S. Department of Energy Chicago Operations Office 9800 S. Cass Avenue, Bldg. 350 Argonne, IL 60439 Attn: C. Boggs-Mayes J. Holm S. Kouba S. Mann J. Roberts
7	U.S. Department of Energy Idaho Operations Office 550 Second Street Idaho Falls, ID 83401 Attn M. Barainca N. Burrell C. Dwight (2) S. Hinschberger T. Rowland J. Solecki
2	U.S. Department of Energy Oak Ridge Operations Office P.O. Box E Oak Ridge, TN 37831 Attn: M. Heiskell S. Oxenbine
3	Battelle Columbus Division 505 King Avenue Columbus, OH 43201-2693 Attn: J. Allen W. Pardue R. Peterson

5 EG&G Idaho, Inc.
P.O. Box 1625
Idaho Falls, ID 83145
Attn: I. Hall (4)
J. Leatham

4 Oak Ridge National Laboratory
P.O. Box X
Oak Ridge, TN 37830
Attn: R. Rawl
T. Rowe
L. Shappert
R. Westfall

1 University of California
Lawrence Livermore National Laboratory
P.O. Box 808
Livermore, CA 94550
Attn: L. E. Fisher

2 Battelle Pacific Northwest Laboratory
Battelle Boulevard
Richland, WA 99352
Attn: G. Beeman
J. Creer

2 Roy F. Weston, Inc.
955 L'Enfant Plaza SW
Washington, DC 20024
Attn: P. Bolton
E. Livingston-Behan

1 ANEFCO, Inc.
904 Ethan Allen Hwy
P.O. Box 433
Ridgefield, CT 06877
Attn: J. Murphy

1 Babcock and Wilcox
Nuclear Equipment Division
91 Stirling Avenue
Barberton, OH 44203
Attn: T. Stevens

1 Chem-Nuclear Systems, Inc.
220 Stoneridge Drive
Columbia, SC 29210
Attn: R. Anderson

1 Combustion Engineering
CE Power Systems
1000 Prospect Hill Road
Windsor, CT 06095
Attn: R. Ng

1 GA Technologies, Inc.
P.O. Box 85608
Building 2, Rm 644
San Diego, CA 92138
Attn: R. Burgoyne

1 Nuclear Assurance Corporation
6251 Crooked Creek Rd.
Norcross, GA 30092
Attn: C. Johnson

1 Nuclear Packaging, Inc.
1010 S. 336th, Suite 220
Federal Way, WA 98003
Attn: R. Haelsig

1 Transnuclear, Inc.
Two Skyline Drive
Hawthorne, NY 10532-2120
Attn: Bill R. Teer

1 Westinghouse Electric Corp.
Waste Technology Services Div.
Box 286
Madison, PA 15663-0286
Attn: S. Little

1 U.S. Council for Energy Awareness
1776 I Street, N.W.
Washington, DC 20006
Attn: J. Siegel

1 Edison Electric Institute
1111 19th Street, N.W.
Washington, DC 20036
Attn: J. Kearney

10 Electric Power Research Institute
P.O. Box 10412
3412 Hillview Avenue
Palo Alto, CA 94304
Attn: R. Lambert
R. Williams (9)

1 Northeast Utilities
P.O. Box 270
Hartford, CT 06101
Attn: R. Bishop

5 LeBoeuf, Lamb, Leiby, and McRae
1333 New Hampshire Avenue, N.W.
Washington, DC 20036
Attn: L. Trosten (5)

1 Utility Nuclear Waste Management Group
1111 19th Street, N.W.
Washington, DC 20036
Attn: J. Davis

3 JNT, Inc.
P.O. Box 1510
Los Gatos, CA 95031-1510
Attn: R. Jones

7 U.S. Nuclear Regulatory Commission
Office of Nuclear Mateials
Safety and Safeguards
Washington, DC 20555
Attn: R. Chappell
A. Grella
R. Odegaarten
C. MacDonald
C. Marotta
J. Roberts
L. Rouse

2 U.S. Nuclear Regulatory Commission
Office of Nuclear Regulatory Research
Washington, DC 20555
Attn: D. Hopkins
W. Lahs

1 U.S. Department of Transportation
Federal Rail Administration
RRS-32
400 7th Street, SW
Washington, DC 20590
Attn: C. Orth

1 U.S. Department of Transportation
Office of Materials Transportation
400-7th Street, S.W.
Washington, DC 20590
Attn: M. Wangler

1 Yankee Atomic Electric Co.
1617 Worcester Rd.
Framington, MA 01701
Attn: V. Pareto

1 Northern States Power Co.
414 Nicollet Mall
Minneapolis, MN 55401
Attn: L. McCarten

1 Wisconsin Electric Power Co.
231 West Michigan St.
Milwaukee, WI 53201
Attn: H. Shimon

1 Southern Company Services
P.O. Box 2625
Birmingham, AL 35202
Attn: K. Folk

2 Duke Power Co.
P.O. Box 33189
Charlotte, NC 28242
Attn: D. Frech
B. Rasmussen

1 Florida Power & Light Co.
P.O. Box 14000
Juno Beach, FL 33408
Attn: D. Brodnick

2 Virginia Power Co.
P.O. Box 2666
Richmond, VA 23261
Attn: J. Fisher
M. Smith

1 Southern California Edison Co.
2244 Walnut Grove Ave.
Rosemead, CA 91770
Attn: J. Ladesich

1 Mr. Douglas Larson, Executive Director
Western Interstate Energy Board
6500 Stapleton Plaza
3333 Quebec Street
Denver, CO 80207
Attn: Ms. Lori Friel

1 Mr. Ken Nemeth, Executive Director
Southern States Energy Board
3091 Governors Lakes Drive
Suite 400
Norcross, GA 30071

1 Ms. Barbara Foster
National Conference of State Legislatures
Energy Science and Natural Resources
1050 17th Street, Suite 2100
Denver, CO 80265

1 Ms. Gail Chehak
National Congress of American Indians
804 D. Street, NE
Washington, DC 20002

1 Ms. Wendy Dixon
U.S. Department of Energy
Nevada Operations Office
P.O. Box 14100
Las Vegas, NV 89114-4100

1 Ms. Beth Darrough
U.S. Department of Energy
Salt Repository Project Office
110 North 25 Mile Avenue
Hereford, TX 79045

1 Mr. Jim Peterson
U.S. Department fo Energy
Richland Operations Office
Basalt Waste Isolation Division
825 Jadwin Avenue
P.O. Box 550
Richland, WA 99352

5 Mr. E. Livesey
British Nuclear Fuel PLC
RISLEY
Warrington WA3 6AS
United Kingdom

5	3141	S. A. Landenberger
3	3151	W. L. Garner
8	3154-1	C. K. Dalin for DOE/OSTI
1	6000	D. L. Hartley
1	6300	R. W. Lynch
1	6320	J. E. Stiegler Attn: TTC Master File
25	6320	TTC Library
1	6321	R. E. Luna
1	6322	J. M. Freedman
10	6322	R. E. Glass
1	6323	G. C. Allen, Jr.
1	8524	P. W. Dean